NEOPLASIA
www.neoplasia.com

Volume 11 Number 11 November 2009 pp. 1216–1225 1216

HE3235 Inhibits Growth of Castration-Resistant Prostate Cancer[1,2]

Theodore D. Koreckij*, Richard J. Trauger†, Robert Bruce Montgomery‡, Tiffany E.M. Pitts*, Ilsa Coleman§, Holly Nguyen*, Chris L. Reading†, Peter S. Nelson§, Robert L. Vessella*,¶ and Eva Corey*

*Department of Urology, University of Washington, Seattle, WA, 98195, USA; †Hollis Eden Pharmaceutical, San Diego, CA 92121, USA; ‡Department of Medicine, University of Washington, Seattle, WA, USA; §Division of Human Biology, Fred Hutchinson Cancer Research Center, Seattle, WA, USA; ¶Puget Sound VA Administrations, Seattle, WA, USA

Abstract

Treatments for advanced prostate cancer (CaP) typically involve androgen deprivation therapy. However, most patients eventually develop castration-resistant CaP (CRPC) for which highly effective therapies are limited. We explored the efficacy of a novel agent, HE3235, in inhibiting growth of CRPC in preclinical models. Castrated male mice were implanted subcutaneously with LuCaP35V CaP xenografts in the presence and absence of 5′-androstenediol (AED) and treated with HE3235. To investigate the effect of HE3235 on CaP tumor in the bone, castrated mice were injected intratibially with C4-2B CaP cells and treated with HE3235. Serum prostate-specific antigen (PSA) levels, tumor volume, immunohistochemistry, gene expression, and levels of intratumoral androgens were analyzed. HE3235 significantly prolonged the tumor doubling time of LuCaP35V, decreased androgen receptor expression, and lowered levels of intratumoral testosterone by ~89% and dihydrotestosterone by ~63% in both the presence and the absence of AED. HE3235 inhibited tumor growth in the bone environment. Weights of tumored tibiae of HE3235-treated animals were lower than those of control ($P = .031$), and normalized PSA levels were also significantly decreased at the end of study by HE3235 treatment ($P = .0076$). HE3235 inhibits the growth of subcutaneous CRPC as well as CRPC in the bone environment. Our data show that HE3235 exhibits a wide range of effects, including alteration of androgen receptor signaling and reductions in levels of intratumoral androgens. Our results support ongoing clinical investigations into the effectiveness of HE3235 in the setting of CRPC and warrants further studies into the mechanisms behind the effects of HE3235.

Neoplasia (2009) 11, 1216–1225

Introduction

Current treatment of advanced prostate cancer (CaP) involves androgen deprivation therapy, but unfortunately, most patients eventually progress to castration-resistant CaP (CRPC). The current criterion standard treatment involves the use of docetaxel-based regimens. Although these regimens offer an improvement in survival over previous therapies for CRPC, the overall survival for these patients still remains only 18 to 20 months [1,2]. Thus, a great deal of emphasis is placed on the development of new, more effective therapies for CRPC.

Although the mechanisms behind development of CRPC are not fully understood, a central theme is that continued activity of the androgen receptor (AR), despite castrate levels of circulating androgens, is critical for tumor growth. There exists a plethora of literature focusing

Abbreviations: AED, 5′-androstenediol; AR, androgen receptor; ARE, androgen response element; BMD, bone mineral density; CaP, prostate cancer; CRPC, castration-resistant prostate cancer; DHT, dihydrotestosterone; IHC, immunohistochemistry; IP, intraperitoneal; PSA, prostate-specific antigen; T, testosterone

Address all correspondence to: Eva Corey, PhD, Department of Urology, Box 356510, University of Washington, Seattle, WA 98195. E-mail: ecorey@u.washington.edu

[1]HE3235 was provided by Hollis Eden Pharmaceuticals, San Diego, CA, and the reagents for prostate-specific antigen determinations were provided by Abbott Laboratories, Abbott Park, IL. The project was funded in part by Hollis Eden Pharmaceuticals. T.K. was supported by the Ruth L. Kirschstein National Research Training Grant.

[2]This article refers to supplementary materials, which are designated by Tables W1 to W3 and are available online at www.neoplasia.com.

Received 5 June 2009; Revised 23 July 2009; Accepted 23 July 2009

DOI 10.1593/neo.09960

on the role of AR in CRPC: AR levels, AR transcriptional complexes, AR mutations, and ligand-independent mechanisms of AR activation (reviewed in [3–5]).

Initially, androgen deprivation therapy focuses on suppression of testicular production of androgens, testosterone (T) and its metabolite, dihydrotestosterone (DHT). The adrenal gland, however, represents an additional source of androgens in humans (i.e., 5′-androstenediol [AED], dehydroepiandrosterone). Adrenal androgens can directly activate AR or be converted to its cognate ligand DHT. Because the synthesis of adrenal androgens is unaffected by treatment methods used to decrease testicular androgen production (i.e., luteinizing hormone-releasing hormone agonists), they are thought to be involved in the growth of CRPC. In support of this hypothesis, secondary hormonal therapies aimed at blocking production of adrenal androgens (i.e., ketoconazole) have resulted in prostate-specific antigen (PSA) declines and delays in disease progression [6]. Further complicating the picture surrounding continued activity of AR in CRPC are the results of recent investigations showing significant levels of intratumoral T and DHT in patients with CRPC. We and others have reported on the continued presence of intratumoral androgens in both xenograft models of CRPC and in metastatic CaP patient samples despite castrate levels of circulating testicular androgens [7,8]. In addition, CaP cells have recently been shown to have *de novo* androgen synthesis capability through upregulation of enzymes involved in steroidogenesis [9]. These data, together with the marginal success of the available secondary hormonal therapies [6], clearly demonstrate the critical need for development of agents that will be more effective at the inhibition of AR signaling. Many new inhibitors of AR signaling are being tested for their efficacy in treating CRPC in preclinical and clinical settings along with several new drugs aimed at blocking specific enzymes in the steroidogenesis pathway [10,11].

We have previously demonstrated that HE3235, a synthetic analog of a naturally occurring androstenediol, inhibits AED-stimulated growth of LNCaP cells *in vitro* and *in vivo* [12]. In the present study, we have evaluated the effects of HE3235 in two models of CRPC: LuCaP35V xenografts grown subcutaneously and C4-2B xenografts grown in the bone environment. Our data show that treatment with HE3235 inhibits the growth rate of subcutaneous CRPC tumors by 25% in animals stimulated with AED and by 43% in animals not stimulated with AED. In addition, HE3235 inhibited the growth of CRPC in the bone environment as demonstrated by a 17% reduction in tibiae weight along with an approximately 50% reduction in normalized PSA levels. The effects of HE3235 include reductions in AR expression, alterations in the AR signaling pathway, and decreases in the levels of intratumoral androgens.

Material and Methods

Cell Lines

LuCaP35V, a CRPC subline of LuCaP 35 CaP xenograft, was derived from the lymph node metastasis of a patient who had previously undergone an orchiectomy [13]. It is maintained by serial passage in castrated severe combined immunodeficient (SCID) male mice. C4-2B, a CRPC subline of LNCaP cells (a gift from Dr. Chung, Emory University), was derived from a bone metastasis [14], and is maintained *in vitro* under standard tissue culture conditions.

Transient Transfection Reporter Assays

For transient transfection, C4-2B cells grown in RPMI 1640 (Invitrogen, Grand Island, NY) supplemented with 10% fetal bovine serum (Atlanta Biological, Atlanta, GA) under standard tissue culture conditions and a single suspension of LuCaP35V cells prepared from tumors [15] were used. Cells were transiently transfected with an androgen response element (ARE) reporter (provided by Dr. Plymate, University of Washington, Seattle, WA) or with a 5.8-kb PSA luciferase plasmid (provided by Dr. Kim, Fred Hutchinson Cancer Research Center, Seattle, WA) using the Amaxa Nucleofector with solution V on program 27 as per the manufacturer's instructions (Amaxa Biosystems, Inc, Gaithersburg, MD). The hTK renilla-luciferase plasmid was transfected under the same conditions to allow for normalization of transfection efficiencies. Control cells were mock-transfected. After transfection, cells were placed in RPMI 1640 with 5% charcoal-stripped serum (Invitrogen) and treated with 0, 10, and 50 nM HE3235. Cells were incubated for 48 hours, and luciferase activity was detected with a Dual-Luciferase Reporter Assay (Promega, Madison, WI) using a Tecan GENios Plus luminometer (Phenix Research Products, Hayward, CA).

Proliferation Study

C4-2B cells were plated in a six-well plate (200,000 cells per well) in RPMI 1640 medium with 5% charcoal-stripped serum, and HE3235 was added at 0, 10, and 50 nM concentrations. After three days, viable cells were counted using the Trypan blue exclusion assay. Experiments were performed in triplicate and repeated twice. Proliferation studies with LuCaP35V were not possible as because this line does not proliferate *in vitro*.

In Vivo *Studies*

All animal procedures were performed in compliance with the University of Washington Institutional Animal Care and Use Committee and National Institutes of Health guidelines. For subcutaneous studies, 50 male CB-17 SCID mice (Charles River Laboratories, Wilmington, MA) were castrated, and after a 2-week recovery period, half of the mice then received subcutaneous AED pellets (5 mg, 60-day time release; IRA, Sarasota, FL). The other half of animals received placebo pellets. LuCaP35V was implanted subcutaneously (~20 mg tumor bits) 3 days after implantation of the pellets. Animals were randomized into the following study groups when tumor volume exceeded 100 mm^3: 1) Control LuCaP35V, group receiving a placebo pellet + placebo treatment (HERF202), n = 12; 2) LuCaP35V + HE3235, group receiving the placebo pellet + HE3235, n = 12; 3) AED-LuCaP35V, group receiving the AED pellet + HERF202, n = 12; and 4) AED-LuCaP35V + HE3235, group receiving the AED pellet + HE3235, n = 11. HE3235, 17α-ethynyl-5α-androstan-3α, 17β-diol (Hollis Eden Pharmaceuticals, Inc, San Diego, CA) was administered through intraperitoneal (IP) injection once daily, 5 d/wk for 4 weeks through IP injection at dose of 160 mg/kg. HE3235 was suspended in Captisol (CyDex, Lenexa, KS) for IP injections to increase bioavailibily. Placebo consisted of Captisol vehicle (HERF202). Tumor volumes were measured twice weekly, and blood samples were drawn weekly for PSA determinations (IMx Total PSA Assay; Abbott Laboratories, Abbott Park, IL). Exponential growth equations were used for calculations of tumor doubling times. Animals were killed after 4 weeks of treatment when tumors exceeded 1000 mm^3 or if otherwise compromised. Sacrifice PSA index was calculated by dividing the serum PSA levels by the tumor volume. At sacrifice, half of each tumor was processed for paraffin embedding and immunohistochemistry (IHC), and the other half was flash frozen for gene expression analysis and determinations of intratumoral androgen levels. Statistical analyses of HE3235 effects were performed using Student's t tests (Prism

GraphPad; GraphPad Software, San Diego, CA). Results with differences yielding $P \le .05$ were considered significant.

For intratibial studies, 30 male CB-17 SCID mice were castrated, and after 2 weeks of recovery, the intratibial injections were performed as previously described [16]. Blood samples were drawn weekly for determination of serum PSA levels, which was used to evaluate tumor growth. When tumors were established in the bone (PSA >0.6 and <5 ng/ml), animals were randomized into two study groups: 1) Control C4-2B, group receiving HERF202, $n = 9$; and 2) C4-2B + HE3235, group receiving HE3235 (160 mg/kg IP), $n = 10$. Animals were dosed daily (IP injections as previously mentioned), 7 d/wk for 4 weeks. Animals were killed after 4 weeks or if otherwise compromised. Tibiae were excised, weighed, decalcified in EDTA, and embedded in paraffin for analyses. Effects of tumor growth and HE3235 treatment on bone was examined using radiographs (Faxitron Specimen Radiography System, Model MX-20; Faxitron x-ray Corporation, Wheeling, IL) and bone mineral density (BMD) measurements (PIXImus Lunar densitometer; GE Healthcare, Waukesha, WI), which were obtained before sacrifice. Statistical analyses were performed using Student's *t* tests (Prism GraphPad; GraphPad Software). Results with differences yielding $P \le .05$ were considered significant.

Determinations of Levels of Intratumoral Androgens

Four animals from each group with LuCaP35V tumors were used for analyses of intratumoral androgens. Levels of intratumoral androgen were determined by mass spectrometry as previously described [8]. Levels of intratumoral androgens were compared using Student's *t* tests, and results yielding $P \le .05$ were considered significant.

RNA Extraction

Tumor fragments (50-100 mg) were placed into 1 ml of STAT-60 solution (Tel-Test, Inc, Friendswood, TX) and homogenized using Omni Tips (Omni International, Marietta, GA). The RNA extraction was carried out as recommended by the manufacturer's protocol.

Gene Expression Profiling and Analysis from Subcutaneous Tumors

For oligo array analyses, we used four pools of RNA from group 1 (control LuCaP35V) and four pools of RNA from group 2 (LuCaP35V + HE3235). Each pool contained an equal amount of RNA from three different tumors from the specific group. A reference standard RNA for use in two-color oligo arrays was prepared as described previously [15]. Total RNA was amplified using the Ambion MessageAmp aRNA Kit (Ambion, Inc, Austin, TX). Amplified amino-allyl RNA from each pooled sample was labeled with Cy3 fluorescent dye (reference amino-allyl RNA was labeled with Cy5) and hybridized to 44K whole human genome expression oligo microarray slides (Agilent Technologies, Inc, Santa Clara, CA).

Fluorescence array images were collected (Agilent DNA oligo array scanner G2565BA, Agilent Technologies, Inc), and Agilent Feature Extraction software was used to grid, extract, and normalize the data. Spots of poor quality or average intensity levels (<300) were removed from further analysis. The Statistical Analysis of Microarray (SAM) program (http://www-stat.stanford.edu/~tibs/SAM/) was used to analyze expression differences between treated and untreated specimens. Unpaired, two-sample *t* tests were calculated for all probes passing filters and controlled for multiple testing by estimation of *q* values using the false discovery rate method. These results were then reduced to unique genes by eliminating all but the highest scoring probe for each gene. Gene set enrichment analysis of GO (http://www.geneontology.org/) categories was performed using the EASE (http://david.abcc.ncifcrf.gov/) software.

Quantitative Reverse Transcription–Polymerase Chain Reaction

Real-time polymerase chain reaction (PCR) confirmation of selected gene expression from the oligo array results was performed as previously described [15]. The same pools of RNA were used as for the oligo array analysis. See Table W1 for primers used to determine expression of genes of interest.

Immunohistochemistry

Five-micrometer sections of paraffin-embedded subcutaneous and intratibial tumors were used. IHC was performed by standard procedure [17], using an anti–human AR mouse monoclonal antibody (1:60 dilution; BioGenex, San Ramon, CA). For analysis, a quasi-continuous score was created by multiplying each nuclear intensity level (1 indicates no stain; 2, faint stain; 3, intense stain) by the corresponding overall percentage of cells at that intensity for the entire tumor, and then totaling the results [18]. All evaluations were blinded, and statistical analysis was performed using Student's *t* tests. IHC for PSA expression in intratibial tumors was done using an anti–human PSA rabbit polyclonal antibody (3 μg/ml; Dako, Carpinteria, CA).

Results

In Vitro *Studies*

Our previous studies with LNCaP cells demonstrated that while HE3235 (Figure 1*A*) inhibits proliferation it stimulates AR-mediated transcription [12]. In the present study, we used castration-resistant C4-2B cells, which express the same mutated AR as LNCaP cells, and LuCaP35V cells, which express wild-type AR. First, we determined if HE3235 alters AR-mediated transcription in these cells using ARE- and PSA-promoter-reporter constructs. Our results show that HE3235 increases AR-mediated transcription using both of the reporter plasmids in C4-2B cells that express mutated AR. AR-mediated transcription was also increased in LuCaP35V that express wild-type AR, but this activation did not reach significance (Figure 1, *B*–*E*). This might be due to a lower transfection efficiency of these cells *in vitro*. There are differences in the magnitude of the increases in AR-mediated transcription between the C4-2B and LuCaP35V cells, and we hypothesize that they might be attributed to the differences of HE3235 effects on mutated and wild-type AR. Important to the intratibial studies, our results also show that treatment with HE3235 causes a significant decrease in the proliferation of C4-2B cells in a dose-dependent fashion (ANOVA, $P < .0001$; Figure 1*F*).

Effect of HE3235 on AED-Supplemented LuCaP35V Subcutaneous Tumors

In the preclinical setting, we first evaluated effects of HE3235 on LuCaP35V in the presence of AED. Castrated male mice were supplemented with AED pellets to closer mimic the human adrenal gland secreting AED because the adrenal gland in mice lacks the enzymes necessary for steroidogenesis [19]. Treatment with HE3235 significantly inhibited growth of LuCaP35V in mice supplemented with AED; doubling time of AED-LuCaP35V + HE3235 was 13.15 ± 2.96 days (mean ± SD) in comparison to 9.87 ± 1.64 days of AED-LuCaP35V ($P = .007$; Figure 2*A*). Treatment with HE3235

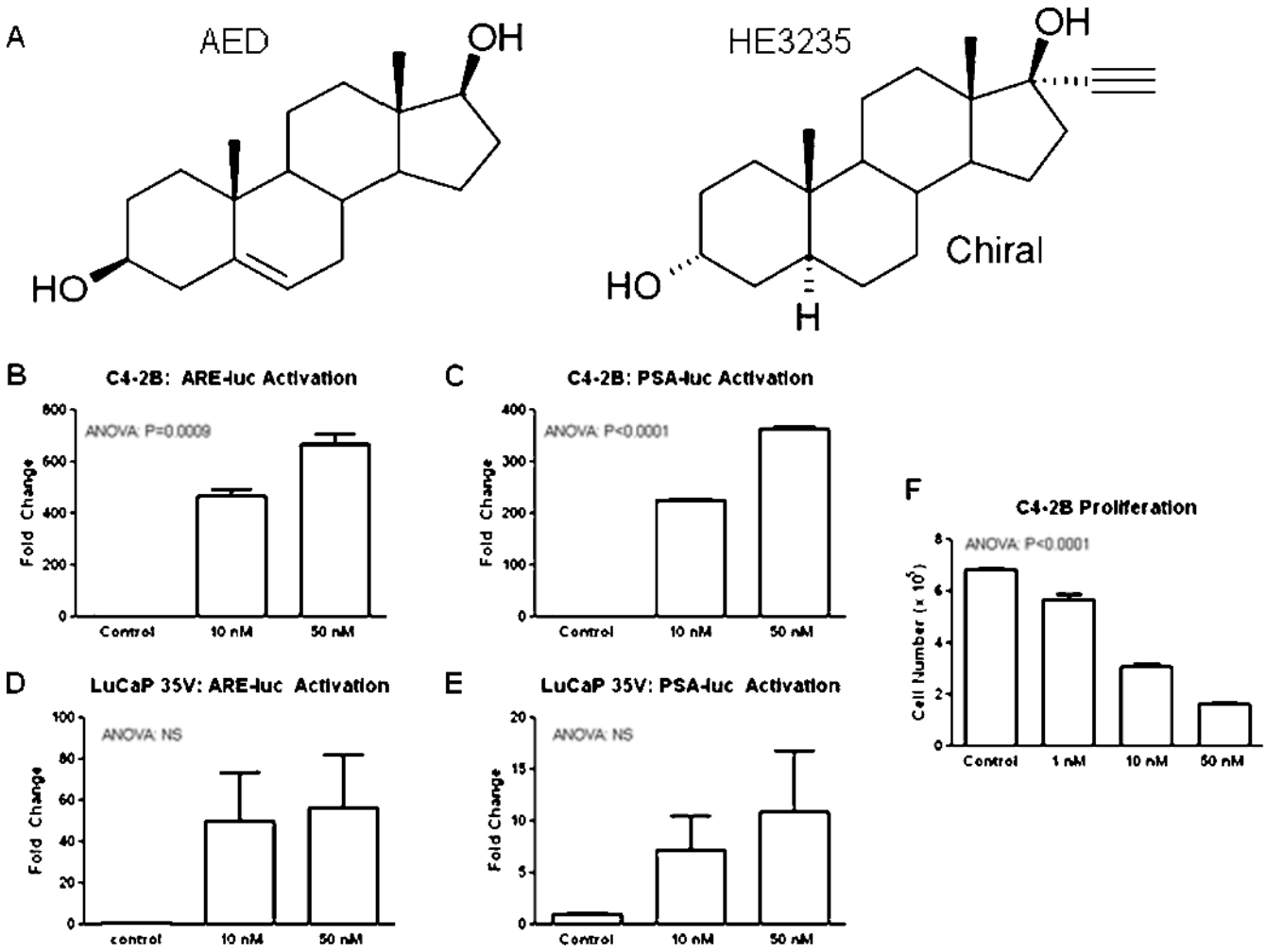

Figure 1. Effects of HE3235 on C4-2B and LuCaP35V cells *in vitro*. (A) Chemical structure of HE3235 and AED. (B and C) HE3235 increased AR-mediated transcription in C4-2B cells *in vitro* as demonstrated by ARE-luc and PSA-promoter-luc reporter assays. C4-2B cells were transfected with ARE-luc (B) or PSA-promoter-luc (C) using Amaxa. After 2 days, the luciferase activity was measured. The luc signal was normalized to renilla luciferase. The results are plotted as fold change over the untreated C4-2B cells. (D and E) Single-cell suspensions of LuCaP 35V cells were prepared by dissociation of subcutaneous tumors. The cells were transfected with ARE-luc (D) or PSA-promoter-luc (E) using Amaxa. Treatment with HE3235 increases AR-mediated transcription in LuCaP35V CaP cells. (F) HE3235 effect on AR-mediated transcription in C4-2B cells. C4-2B cells were grown under standard tissue culture conditions (see Materials and Methods) and treated with HE3235. HE3235 significantly inhibited C4-2B proliferation. *RLU* indicates relative light units.

also resulted in slight increases in serum PSA levels *versus* the control AED-LuCaP35V animals, but these differences did not reach significance. Similarly, the PSA index at the end of the study was also higher in HE3235-treated animals, and this difference did not reach significance (AED-LuCaP35V, 0.09 ± 0.04 ng/ml per cubic millimeter; and AED-LuCaP35V + HE3235, 0.13 ± 0.09 ng/ml per cubic millimeter, $P = .17$). However, these elevations in PSA are in concordance with the above *in vitro* studies demonstrating increases in AR-mediated transcription by HE3235 treatment.

Effect of HE3235 on LuCaP35V Subcutaneous Tumors

Our previous data showed that HE3235 inhibits proliferation of LNCaP cells in the presence and absence of AED *in vitro* [12]. Therefore, in this study, we set out to investigate whether HE3235 inhibits growth of CaP tumors in castrated male mice in the absence of AED. These experimental conditions mimic the clinical scenario of patients treated with agents aimed at blocking adrenal synthesis of androgens (e.g., ketoconazole). In this setting, HE3235 significantly inhibited the tumor doubling times of LuCaP35V (LuCaP35V + HE3235, 18.2 ± 6.28 days; untreated LuCaP35V, 10.44 ± 1.8 days; $P < .0001$; Figure 2*B*). HE3235 treatment resulted in significant increases in serum PSA levels in the treated animals *versus* control animals bearing LuCaP35V tumors in the period of 1 to 3 weeks after treatment initiation ($P < .0001$; Figure 2*B*). PSA levels were not significantly higher in the treated animals at the end of the study. We hypothesize that this is due to the decreases in tumor volume. This explanation is supported by results showing a significantly higher PSA index in the LuCaP35V + HE3235 animals than PSA index in the LuCaP35V animals, 0.18 ± 0.07 *versus* 0.07 ± 0.02 ng/ml per cubic millimeter, respectively ($P < .0001$).

Effects of HE3235 on the Growth of CaP in Bone

To investigate the effect of HE3235 on CRPC tumors growing in the bone environment, we used C4-2B cells directly injected into

murine bone. We selected C4-2B cells for these experiments because they exhibit a mixed osteoblastic/osteolytic response when grown in the bone environment similar to that seen in patients with CaP bone metastases. Our results show that HE3235 treatment resulted in a decreased weight of tumored tibiae in comparison to control tumored tibiae (0.056 ± 0.004 *vs* 0.068 ± 0.015 g, $P = .031$; Figure 3*A*), suggesting smaller tumor volume and/or lower amount of bone. The weight of the HE3235-treated tumored tibiae was not significantly different from that of the contralateral nontumored tibiae of the same animals. In contrast to the previously mentioned study with LuCaP35V, HE3235 treatment resulted in decreases of serum PSA in this model. When normalized to enrollment, HE3235 initially increased serum PSA levels (trend: $P < .1$), whereas at weeks 3 and 4, significant decreases were detected (Figure 3*A*). Because the serum PSA levels were lower in animals with HE3235-treated C4-2B tumors *versus* animals with control C4-2B tumors, we next examined the effects of HE3235 treatment on the bone. Our results show that C4-2B cells decreased BMD of the tibiae, and despite the lower tumor burden, no differences in BMD were detected between HE3235-treated *versus* control C4-2B tumored tibiae (0.05 ± 0.004 *versus* 0.049 ± 0.004 g/cm^2, $P = .65$; Figure 3*A*).

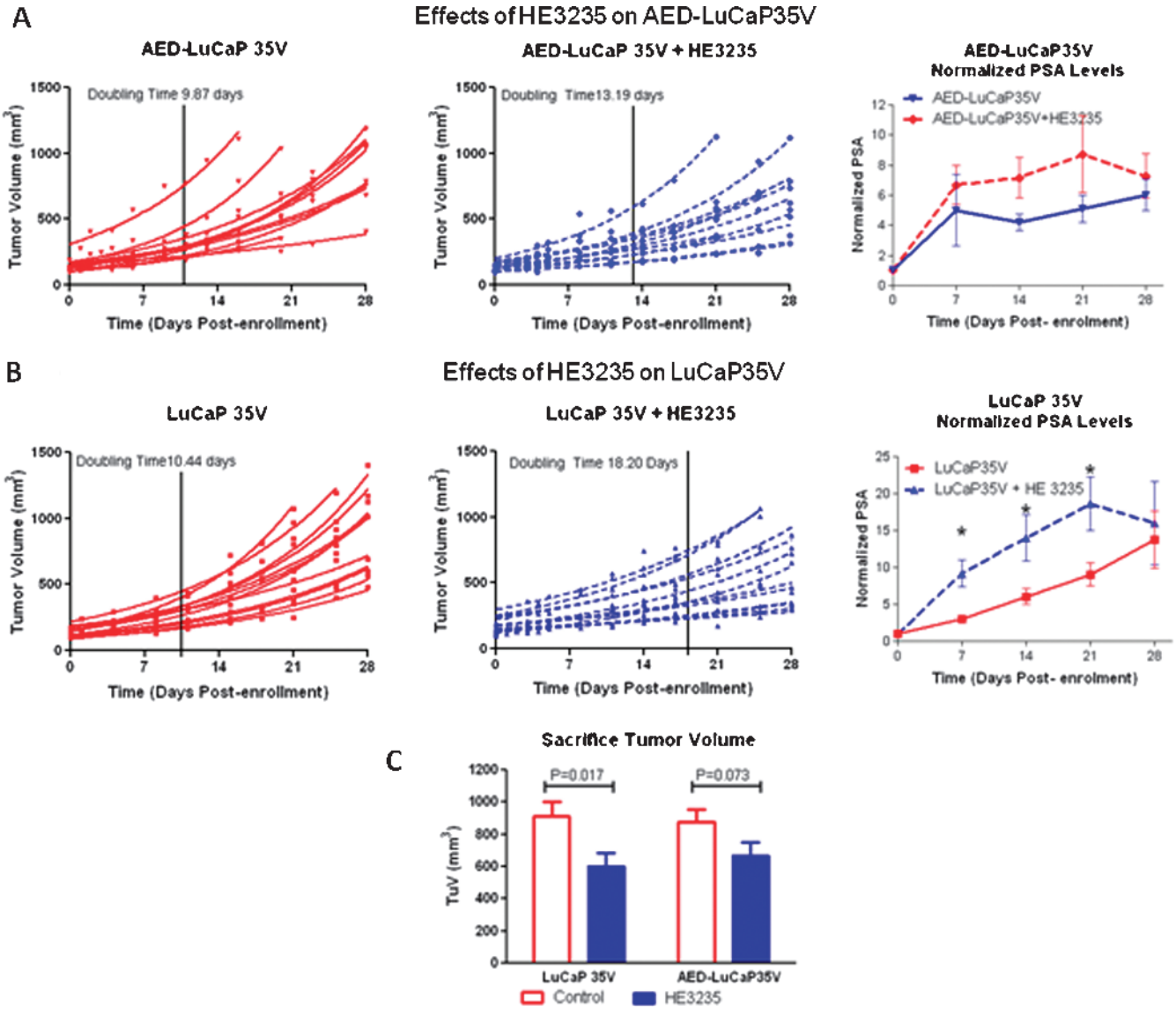

Figure 2. Effects of HE3235 on LuCaP35V *in vivo*. (A) HE3235 inhibited growth of AED-supplemented LuCaP35V subcutaneous tumors (25% inhibition, $P = .007$), whereas PSA levels were slightly but not significantly increased during the study. LuCaP35V tumors were grown subcutaneously in AED-supplemented animals. When tumors reached 100 mm^3, the animals were randomized between two groups; control and HE3235-treated groups (HE3235: 160 kg/kg 5 d/wk). The doubling times were calculated for each individual tumor using exponential growth curve for determinations of average doubling times (line represents average doubling time per group). Left panel — control tumors, middle panel — HE3235-treated tumors, right panel — HE3235 treatment effects on serum PSA levels (values are normalized to enrollment). (B) HE3235 inhibited growth of LuCaP35V subcutaneous tumors (43% inhibition, $P < .0001$), whereas PSA levels were significantly increased at weeks 2 to 3 of the treatment. Left panel — control tumors, middle panel — HE3235-treated tumors, right panel — serum PSA levels (values are normalized to enrollment). (C) Tumor volume at sacrifice was significantly decreased by HE3235 treatment in castrated male animals with and without AED supplementation.

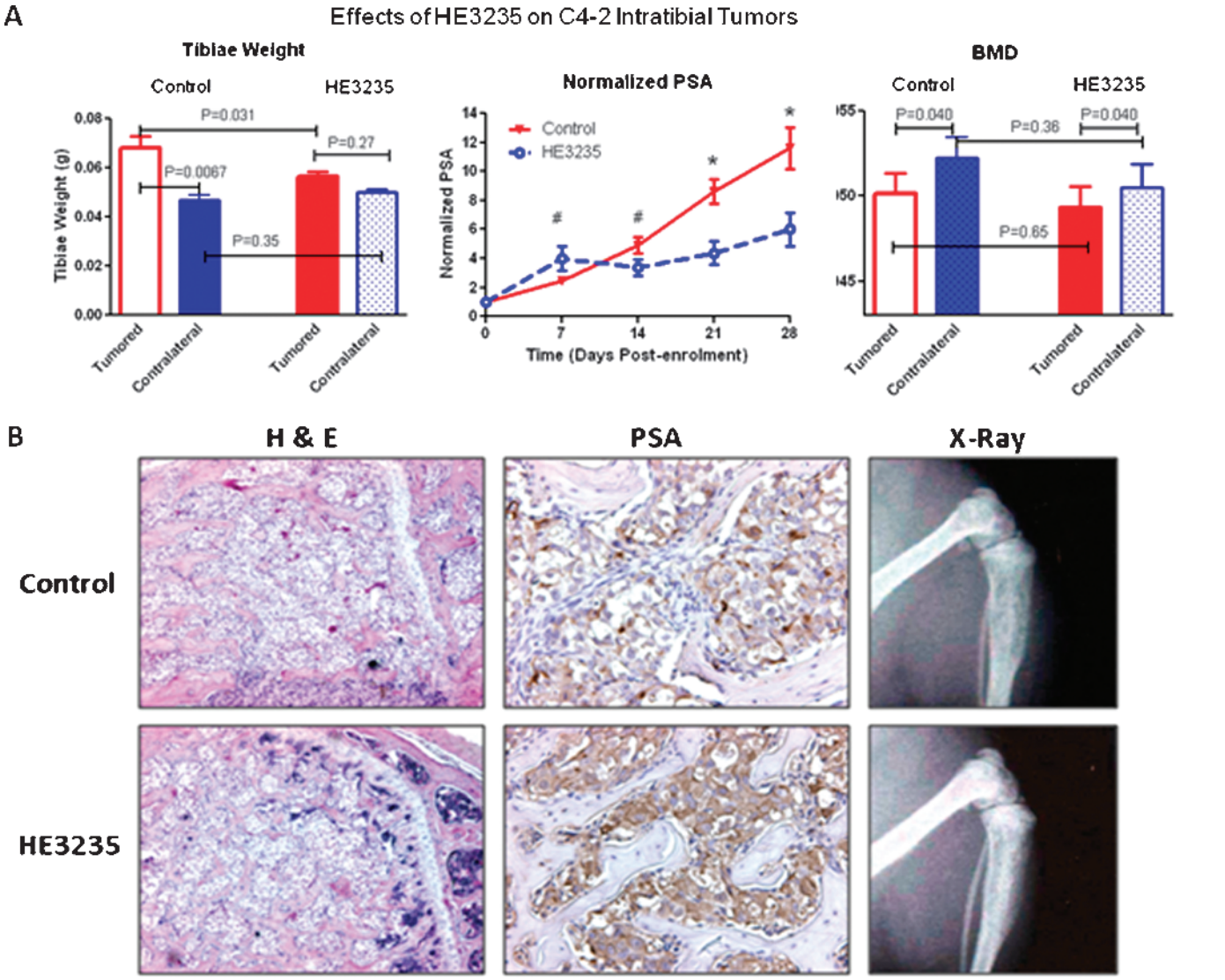

Figure 3. Effect of HE3235 on growth of C4-2B in bone. (A) C4-2B cells were injected into tibiae of castrated male mice and when tumors were established half of the animals were treated with HE3235 (160 mg/kg) daily for 28 days. Left panel — HE3235 treatment resulted in decreases in weight of tumored tibiae suggesting inhibition of tumor growth while not exhibiting any significant effects on nontumored tibiae. Furthermore, HE3235-treated tumored tibiae weight was not significantly different as contralateral nontumored tibiae. Middle panel — HE3235 treatment caused alterations in serum PSA levels, which were significantly decreased at weeks 3 and 4 of the treatment (values are normalized to enrollment). $^{*}P < .001$, $^{\#}P < .10$. Right panel — HE3235 treatment did not have any significant effects on BMD of tumored and nontumored tibiae. BMD was measured at the site of tumor-cell injection adjacent to the growth place. (B) Representative examples of H&E, PSA immunoreactivity, and radiographs of HE3235-treated and control tibiae are shown. Left panel — H&E staining show tumor growth in the bone marrow cavity next to the growth plate (located on the right-hand side). Multiple tumor foci are present between bone trabeculae secondary to the growth of this tumor in bone (magnification, ×10). Middle panel — HE3235-treated tibiae show intensive PSA immunoreactivity (brown staining) in comparison to untreated tumored tibiae. Right panel — representative radiographs of tibia from each group.

Also, no differences in BMD were detected between normal contralateral tibiae of the two groups (Figure 3*A*).

Representative radiographs and hematoxylin and eosin (H&E) staining of the tumored tibiae are shown in Figure 3*B*. These images show an osteoblastic reaction associated with growth of C4-2B tumors in bone and tumor foci between newly formed woven bone in both HE3235-treated and control tibiae (Figure 3*B*). We have also performed IHC analysis of PSA expression. Our results show that HE3235-treated tumor exhibited stronger PSA immunoreactivity despite lower levels of serum PSA (Figure 3*B*).

Analysis of Intratumoral Androgens in LuCaP35V Subcutaneous Tumors

We have previously shown that there are detectable levels of intratumoral androgens in CRPC xenografts and in human CRPC samples despite anorchid levels of circulating androgens [8]. Thus, we set out to determine whether the HE3235 inhibitory effects involve alterations in levels of intratumoral androgens. Treatment with HE3235 significantly lowered levels of T and DHT in LuCaP35V tumors both in the presence and in the absence of AED when compared with respective control animals (Table 1). Animals receiving HE3235 with AED

Table 1. Intratumoral Androgen Levels in LuCaP35V Subcutaneous Tumors.

Androgens	AED-LuCaP35V	AED-LuCaP35V + HE3235	Control LuCaP35V	LuCaP35V + HE3235
T (pg/mg)	2.90 ± 0.31	1.06 ± 0.35	1.47 ± 0.67	0.10 ± 0.05
DHT (pg/mg)	3.03 ± 0.65	1.81 ± 0.31	4.28 ± 1.04	0.64 ± 0.17

Values are mean ± SD.

supplementation had a 63% reduction in T levels in tumors *versus* control AED-supplemented tumors ($P < .001$), and a 40% reduction in DHT levels ($P = .015$). Interestingly, HE3235 caused even larger reductions in levels of intratumoral androgens in tumors growing in castrated animals not supplemented with AED. T levels were 93% lower in LuCaP35V + HE3235 *versus* control LuCaP35V tumors ($P = .006$), and DHT levels were reduced by 85% in HE3235-treated LuCaP35V in comparison to control LuCaP35V tumors ($P < .001$). Owing to the small size of intratibial tumors, we were unable to determine the intratumoral androgen levels in these specimens.

Gene Expression Analysis of LuCaP35V Subcutaneous Tumors

In an attempt to delineate in more detail the mechanisms of HE3235 effects on CRPC, we set out to investigate alteration in RNA expression levels in LuCaP35V tumors, which resulted from HE3235 treatment. We performed gene expression analysis on control LuCaP35V and LuCaP35V + HE3235 groups because HE3235 proved most efficacious in this experimental setting. To compare the overall expression patterns of control LuCaP35V and HE3235-treated LuCaP35V tumors on oligo arrays, $\log_2$ ratio measurements were analyzed using the SAM software to perform an unpaired two-sample *t* test (http://www-stat.stanford.edu/_tibs/SAM/). A false discovery rate of *q* values less than 5% was considered significant and set the threshold for differential expression at greater than a 1.6-fold change with treatment. At this level of significance, there were 355 unique genes upregulated and 30 unique genes downregulated in HE3235-treated LuCaP35V *versus* control LuCaP35V. An EASE gene set enrichment revealed significant changes in a multitude of cellular pathways associated with various biologic processes. Owing to our previous findings that HE3235 stimulates AR-mediated transcription as determined by reporter assay [9], and our present results demonstrating the effects of HE3235 on levels of intratumoral androgens, we focused further investigations on alterations associated with AR-mediated transcription and on enzymes involved in steroidogenesis. Our results show that 67 of 355 HE3235-upregulated and 8 of 30 HE3235-downregulated messages have been previously reported to be regulated by androgens (Table W2), whereas the analysis of expression levels of selected enzymes associated with the steroidogenesis pathway (Table W3) did not reveal any significant changes fitting the previously mentioned criteria. The oligo array analysis also showed that AR messenger RNA (mRNA) levels were significantly decreased by HE3235 treatment (–3.1-fold).

We used real-time PCR to validate some of the oligo array results. We have elected two of the most downregulated genes, *AR* and *AK5*; five highly upregulated AR-regulated genes with suggested roles in CaP progression; and we also included *PSA* and *hK2*, two well-known AR-regulated genes that did not show altered expression on oligo arrays. Real-time PCR confirmed the oligo array analysis results showing significant down-regulation of *AR* and *AK5* mRNA in HE3235-treated tumors as well as the up-regulation of several AR-regulated genes, although not all genes examined resulted in statistically significant changes. In animals supplemented with AED, we observed a diminished and in some instances, an abolished effect on gene expression in response to HE3235 (Figure 4). Despite the fact that the oligo array analysis did not show any significant alteration in expression of 13 enzymes associated with steroidogenesis, we examined levels of three of these, HSD17B3, AKR1C3, and SRD5A1 by PCR. Even this analysis did not reveal any significant alterations in mRNA levels of these enzymes after HE3235 treatment (data not shown).

Effects of HE3235 on AR Immunoreactivity

The results of the oligo arrays and real-time PCR results showed that levels of AR transcript were decreased by treatment with HE3235. Therefore, the effects of HE3235 on levels of AR protein were investigated. IHC analysis showed significant decreases in the nuclear localization of AR after HE3235 treatment; the AR score of LuCaP35V + HE3235 was 248 ± 8 *versus* 198 ± 28 of control ($P = .0048$), whereas alteration of the AR score in AED-LuCaP35V + HE3235 *versus* AED-LuCaP35V did not reach significance (228 ± 36 *vs* 208 ± 8, $P = .28$; Figure 5). The AR score of HE3235-treated C4-2B intratibial tumors was also significantly lower *versus* control C4-2B tumors (236 ± 15 *vs* 182 ± 15, $P < .001$; Figure 5).

Discussion

We have recently reported that HE3235 inhibits growth of AED-stimulated LNCaP cells *in vitro* and *in vivo* [12]. However, LNCaP cells are androgen-sensitive and express a mutated AR. Despite the relatively high frequency of mutations in AR reported in CRPC, which can alter AR responses to various steroids, most CRPC tumors express wild-type AR [20]. Therefore, to further support the clinical potential of this compound, our first objective was to determine whether HE3235 inhibits growth of CRPC LuCaP35V cells that express wild-type AR. Our results clearly demonstrate that HE3235 inhibits growth of CRPC cells that express wild-type AR and that HE3235 inhibits growth of LuCaP35V not only in the presence of AED but also in the absence of AED. Interestingly, the inhibition was even more pronounced when AED was absent. Although the mechanisms behind these differences in tumor growth are not known at present, our results indicate that in a clinical setting, HE3235 might have more beneficial effects when used in men on secondary androgen ablation regimens that include inhibitors of adrenal androgen synthesis. However, despite the inhibition of growth, HE3235 did not eradicate the tumors, but merely slowed down tumor growth. Further studies are needed to determine if higher doses of HE3235 or more frequent administration would result in the elimination of the tumors.

Serum PSA levels are used to monitor disease progression as well as effectiveness of treatment. HE3235 treatment of animals bearing LuCaP35V tumors resulted in increases of serum PSA and in PSA index despite the inhibition of tumor growth. In concordance with

these *in vivo* results, we also show that AR-mediated transcription was increased by HE3235 *in vitro* using ARE- and PSA-promoter-reporter assays, further supporting stimulation of AR-mediated transcription despite growth inhibition. Because inhibition of tumor growth along with increases in AR-mediated transcription is not well documented in the literature, we further evaluated this negative association by oligo array analysis, which confirmed increases in AR-mediated transcription based on higher levels of messages which expression is regulated by AR. To further complicate the situation of decreased tumor volume, increased serum PSA, and increased levels of multiple AR-regulated genes, HE3235 treatment decreased the expression of the AR mRNA and lowered levels of nuclear AR in the HE3235-treated tumors. More detailed investigations of the effects of HE3235 on tumor growth and AR-mediated transcription will be required to fully understand this interplay regulation of tumor growth and AR signaling. However, we currently have two working hypotheses: 1) levels of HE3235 in the tumors are sufficient to cause increases in AR-mediated transcription despite lower levels of AR and lower intratumoral androgens and 2) other mechanisms, independent of AR, are involved in stimulation of expression of AR-regulated genes. For example, it has recently been reported that mitogen-activated protein kinase pathway stimulates ARE-reporter activity in PC-3 and DU 145 cells that lack AR [21].

One of the important recent findings in CaP research is that there are measurable levels of intratumoral androgens in CRPC tumors despite anorchid levels of serum androgens [8]. Abiraterone, a novel inhibitor of steroidogenesis currently evaluated in preclinical and clinical settings, reduces serum androgens in patients and may function by suppressing intratumoral androgens in CRPC [10,22]. Therefore, we examined whether the inhibition of tumor growth by HE3235 is also associated with altered levels of intratumoral

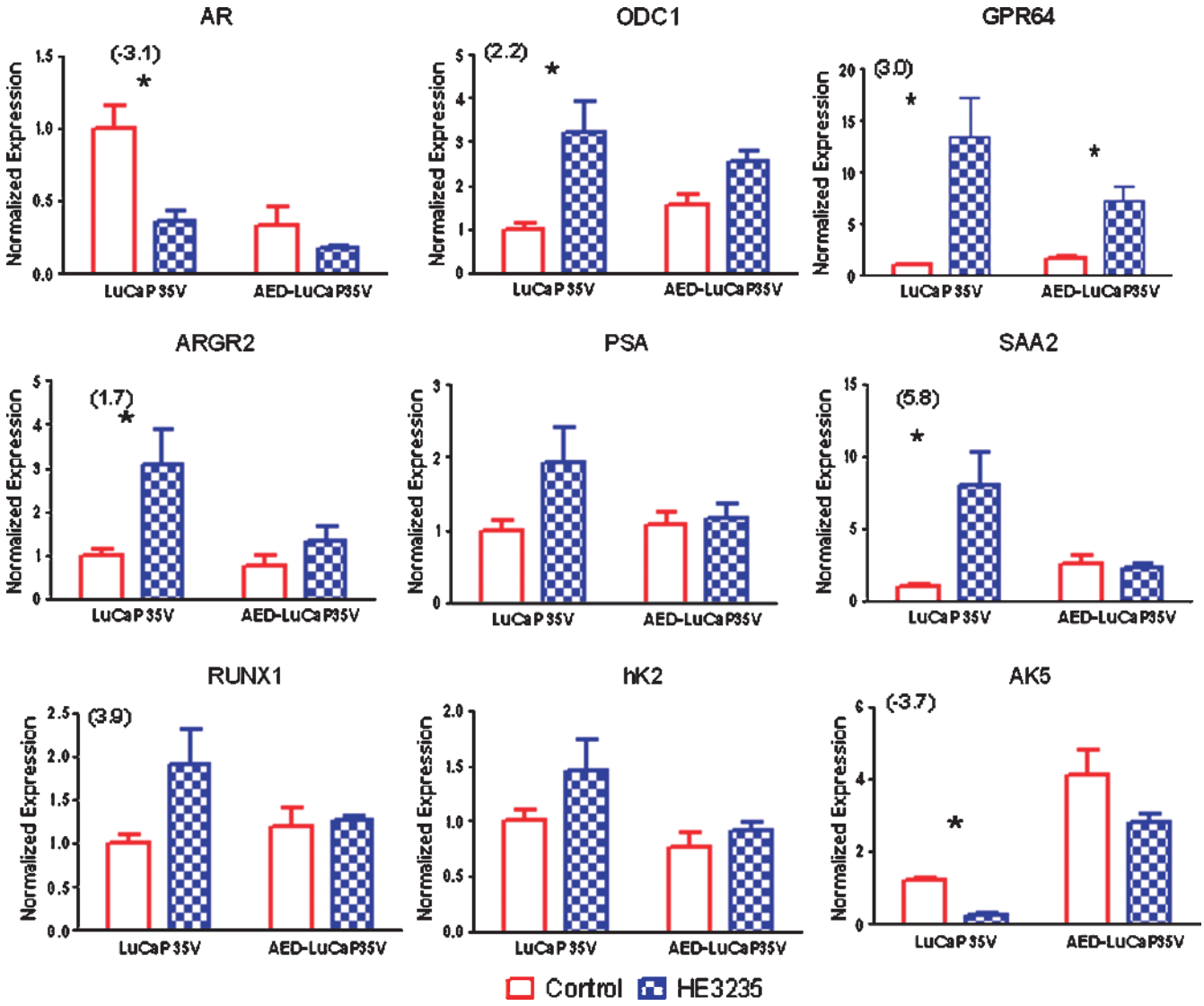

Figure 4. Real-time PCR validation of the androgen-regulated genes that demonstrated response to treatment with HE3235 on oligo array analysis. We confirmed AR down-regulation concomitantly with AR activation as demonstrated by differential changes in AR-regulated genes. The addition of AED seems to attenuate the effect of HE3235 on these genes. *ODC1* indicates ornithine decarboxylase 1; *GPR64*, G protein–coupled receptor 64; *ARG2*, anterior gradient homolog 2 (*Xenopus laevis*); *SAA2*, serum amyloid A2; *RUNX1*, runt-related transcription factor 1; *hK2*, human glandular kallikrein; *AK5*, adenylate kinase 5. Numbers in parentheses show fold change in oligo array analysis. Significant differences were detected in number of mRNA in LuCaP35V treated with HE3235 *versus* control tumors. *$P < .05$.

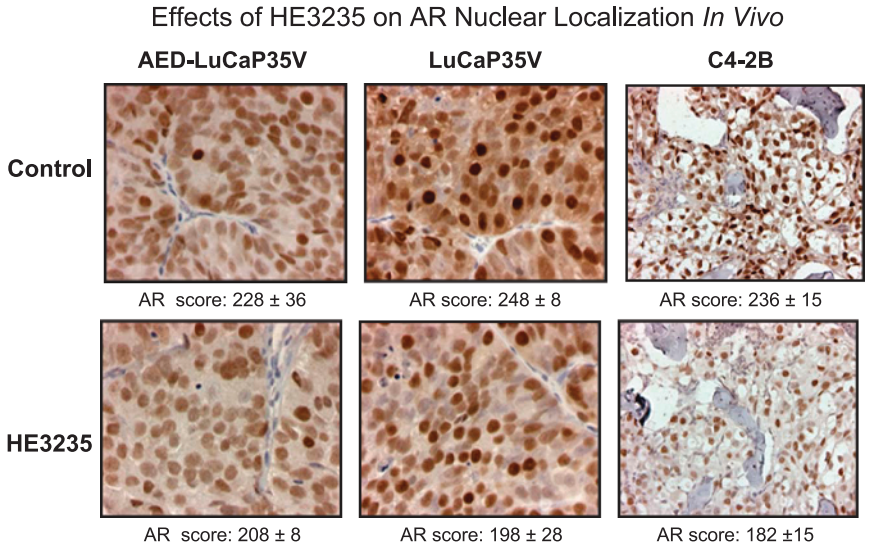

Figure 5. Effects of HE3235 on AR immunoreactivity. Sections of treated and control tumors (AED-LuCaP35V and LuCaP35V subcutaneous tumors and C4-2B intratibial tumors) were stained with anti-AR antibody, and nuclear staining was quantified based on intensity of immunoreactivity and percentage of positive nuclei. HE3235 significantly decreased the AR score in LuCaP 35V and C4-2B tumors, although the decreases were not significant in AED-LuCaP35V. Original magnification: AED-LuCaP35V and LuCaP 35V, ×20; C4-2B, ×10.

androgens. In both non-AED and AED-supplemented animals, HE3235 treatment resulted in significant reductions in intratumoral T and DHT. A greater suppression of intratumoral androgens was detected in LuCaP35V + HE3235 tumors *versus* tumors grown in the presence of AED. These differences might be instrumental in the less pronounced inhibition of growth in AED-supplemented tumors. One potential mechanism resulting in decreased levels of intratumoral androgen might be HE3235 inhibition of the transcription of enzymes involved in steroidogenesis because increased messages have been detected in CRPC metastases [8]. However, despite decreased levels of intratumoral androgens, HE3235 did not alter the transcription of selected enzymes associated with steroidogenesis. Nonetheless, transcriptional control does not represent the only means by which to control intratumoral androgen production. HE3235 suppression of T and DHT in all tumors may be the result of either a blockade on import of androgenic precursors or inhibition of enzymatic activity of the components of the steroid synthesis pathway. The exact mechanism behind this suppression of intratumoral androgens is not known, and delineation of the mechanism(s) will require further investigations on HE3235's effect on enzyme activity *in vitro* and on transporters of androgens and their precursors (e.g., SLCO1B3 and SLCO2B1).

Even with dramatic reductions in the levels of intratumoral androgens, LuCaP35V tumors were not eliminated. Their growth was merely slowed. This may indicate either of the following: 1) the low levels of intratumoral androgens still present in LuCaP35V + HE3235 tumors are sufficient to drive CRPC tumor growth and greater reductions in levels of intratumoral androgens will be necessary for complete inhibition of growth; or 2) a subset of truly castration-resistant tumor cells exist in these tumors that do not require androgens for growth. Therefore, as new agents aimed at blocking the intracrine synthesis of androgens become available, improvements in patient outcomes must be tempered against how much suppression of intratumoral androgen production is achieved, and drugs aimed at decreasing expression of AR as well as agents that will kill AR-negative cells need to be developed and evaluated.

One of the most frequent sites of CaP metastases is bone [16]. It is important that new pharmaceuticals aimed at treating advanced CaP are tested against CaP growing within the bone environment. Our results show that HE3235 inhibits the growth of CRPC in bone as demonstrated by decreased tibiae weight as well as decreased serum PSA levels in HE3235-treated animals. The decreases in serum PSA levels are interesting. We have shown *in vitro* that HE3235 increases AR-mediated transcription in both C4-2B and LuCaP35V cells using reporter assay, and we show increased serum PSA levels *in vivo* with subcutaneous LuCaP35V tumors treated with HE3235. However, serum PSA levels in our intratibial studies were decreased by the HE3235 treatment. We hypothesize that because treated tumors are producing more PSA, an even greater reduction in tumor volume is necessary before serum PSA values decrease in comparison to control tumors. Serum PSA increases caused by HE3235 treatment of larger subcutaneous tumors initially overshadows the concomitant inhibition of tumor growth. In the intratibial study, treatment is started on considerably smaller enrollment tumor volumes that are more susceptible to growth inhibition. With smaller enrollment tumor volumes in the intratibial study, the balance between HE3235 effects on AR-mediated transcription and inhibition of tumor growth is reached sooner as is demonstrated by the initial elevation of serum PSA levels in HE3235-treated animals followed by lower levels thereafter. Our *in vitro* experiments, demonstrating HE3235 inhibition of C4-2B proliferation taken together with our IHC analysis showing activity of HE3235 within the bone environment, further support the premise that HE3235 inhibits CRPC growth within the bone.

In conclusion, our results show that HE3235 inhibits growth of CRPC in multiple models of CaP, including inhibition of CRPC in the bone environment. It invokes a variety of cellular alterations contributing to its ability to inhibit growth of CaP cells, including decreases in levels of AR messages and AR nuclear localization as well as inhibition of the production of intratumoral androgens. Our results warrant further investigation into mechanisms of HE3235 action and clinical investigation of HE3235 in the treatment of CRPC.

Acknowledgments

The authors thank Lisha Brown and Ted Kalhoun for their technical expertise.

References

[1] Petrylak DP, Tangen CM, Hussain MH, Lara PN Jr, Jones JA, Taplin ME, Burch PA, Berry D, Moinpour C, Kohli M, et al. (2004). Docetaxel and estramustine compared with mitoxantrone and prednisone for advanced refractory prostate cancer. *N Engl J Med* **351**, 1513–1520.

[2] Tannock IF, de WR, Berry WR, Horti J, Pluzanska A, Chi KN, Oudard S, Theodore C, James ND, Turesson I, et al. (2004). Docetaxel plus prednisone or mitoxantrone plus prednisone for advanced prostate cancer. *N Engl J Med* **351**, 1502–1512.

[3] Burnstein K (2005). Regulation of androgen receptor levels: implications for prostate cancer progression and therapy. *J Cell Biochem* **95**, 657–669.

[4] Culig Z, Comuzzi B, Steiner H, Bartsch G, and Hobisch A (2004). Expression and function of androgen receptor coactivators in prostate cancer. *J Steroid Biochem Mol Biol* **92**, 265–271.

[5] Scher HI, Buchanan G, Gerald W, Butler LM, and Tilley WD (2004). Targeting the androgen receptor: improving outcomes for castration-resistant prostate cancer. *Endocr Relat Cancer* **11**, 459–476.

[6] Lam JS, Leppert JT, Vemulapalli SN, Shvarts O, and Belldegrun AS (2006). Secondary hormonal therapy for advanced prostate cancer. *J Urol* **175**, 27–34.

[7] Titus MA, Schell MJ, Lih FB, Tomer KB, and Mohler JL (2005). Testosterone and dihydrotestosterone tissue levels in recurrent prostate cancer. *Clin Cancer Res* **11**, 4653–4657.

[8] Montgomery RB, Mostaghel EA, Vessella R, Hess DL, Kalhorn TF, Higano CS, True LD, and Nelson PS (2008). Maintenance of intratumoral androgens in metastatic prostate cancer: a mechanism for castration-resistant tumor growth. *Cancer Res* **68**, 4447–4454.

[9] Locke JA, Guns ES, Lubik AA, Adomat HH, Hendy SC, Wood CA, Ettinger SL, Gleave ME, and Nelson CC (2008). Androgen levels increase by intratumoral *de novo* steroidogenesis during progression of castration-resistant prostate cancer. *Cancer Res* **68**, 6407–6415.

[10] Attard G, Reid AH, Yap TA, Raynaud F, Dowsett M, Settatree S, Barrett M, Parker C, Martins V, Folkerd E, et al. (2008). Phase I clinical trial of a selective inhibitor of CYP17, abiraterone acetate, confirms that castration-resistant prostate cancer commonly remains hormone driven. *J Clin Oncol* **26**, 4563–4571.

[11] Vasaitis T, Belosay A, Schayowitz A, Khandelwal A, Chopra P, Gediya LK, Guo Z, Fang HB, Njar VC, and Brodie AM (2008). Androgen receptor inactivation contributes to antitumor efficacy of 17α-hydroxylase/17,20-lyase inhibitor 3β-hydroxy-17-(1*H*-benzimidazole-1-yl)androsta-5,16-diene in prostate cancer. *Mol Cancer Ther* **7**, 2348–2357.

[12] Trauger R, Corey E, Bell D, White S, Garsd A, Stickney D, Reading C, and Frincke J (2009). Inhibition of androstenediol-dependent LNCaP tumour growth by 17α-ethynyl-5α-androstane-3α, 17β-diol (HE3235). *Br J Cancer* **100**, 1068–1072.

[13] Corey E, Quinn JE, Buhler KR, Nelson PS, Macoska JA, True LD, and Vessella RL (2003). LuCaP 35: a new model of prostate cancer progression to androgen independence. *Prostate* **55**, 239–246.

[14] Thalmann GN, Sikes RA, Wu TT, Degeorges A, Chang SM, Ozen M, Pathak S, and Chung LW (2000). LNCaP progression model of human prostate cancer: androgen-independence and osseous metastasis. *Prostate* **44**, 91–103.

[15] Coleman IM, Kiefer JA, Brown LG, Pitts TE, Nelson PS, Brubaker KD, Vessella RL, and Corey E (2006). Inhibition of androgen-independent prostate cancer by estrogenic compounds is associated with increased expression of immune-related genes. *Neoplasia* **8**, 862–878.

[16] Corey E, Quinn JE, Bladou F, Brown LG, Roudier MP, Brown JM, Buhler KR, and Vessella RL (2002). Establishment and characterization of osseous prostate cancer models: intra-tibial injection of human prostate cancer cells. *Prostate* **52**, 20–33.

[17] Kiefer JA, Vessella RL, Quinn JE, Odman AM, Zhang J, Keller ET, Kostenuik PJ, Dunstan CR, and Corey E (2004). The effect of osteoprotegerin administration on the intra-tibial growth of the osteoblastic LuCaP 23.1 prostate cancer xenograft. *Clin Exp Metastasis* **21**, 381–387.

[18] Lai JS, Brown LG, True LD, Hawley SJ, Etzioni RB, Higano CS, Ho SM, Vessella RL, and Corey E (2004). Metastases of prostate cancer express estrogen receptor-beta. *Urology* **64**, 814–820.

[19] van Weerden WM, Bierings HG, van Steenbrugge GJ, de Jong FH, and Schroder FH (1992). Adrenal glands of mouse and rat do not synthesize androgens. *Life Sci* **50**, 857–861.

[20] Marcelli M, Ittmann M, Mariani S, Sutherland R, Nigam R, Murthy L, Zhao Y, DiConcini D, Puxeddu E, Esen A, et al. (2000). Androgen receptor mutations in prostate cancer. *Cancer Res* **60**, 944–949.

[21] Carey AM, Pramanik R, Nicholson LJ, Dew TK, Martin FL, Muir GH, and Morris JD (2007). Ras-MEK-ERK signaling cascade regulates androgen receptor element–inducible gene transcription and DNA synthesis in prostate cancer cells. *Int J Cancer* **121**, 520–527.

[22] Montgomery RB, Mostaghel E, Nelson PS, Marck B, Nguyen H, and Vessella RL (2009). Abiraterone suppresses castration resistant human prostate cancer growth in the absence of testicular and adrenal androgens. *Advances in Prostate Cancer, AACR Conference, January 2009.* San Diego, CA, Abstract.

Table W1. Real-time PCR Primers.

17BHSD3	Hydroxysteroid (17-beta) dehydrogenase 3	5′: CTGAAGCTCAACACCAAGGTCA 3′: CTGCTCCTCTGGTCCTCTTCAG	NM_000197
AR	Androgen receptor	5′: GGACTTGTGCATGCGGTACTCA 3′: CCTGGCTTCCGCAACTTACAC	NM_000044
AGR2	Anterior gradient homolog 2 (*Xenopus laevis*)	5′: GTCCCCAGGATTATGTTTGTTGACC 3′: AGTCTTCTCACACTTCTTCTGGTTTC	NM_006408
AK5	Adenylate kinase 5	5′: GGAGGTGAAGCAAGGGGAAGAGTT 3′: TCCTTTGGAGAAGGCGGTTGGTC	NM_174858.1
AKR1C3	Aldo-keto reductase family 1, member C3	5′: GAGAAGTAAAGCTTTGGAGGTCACA 3′: CAACCTGCTCCTCATTATTGTATAA	NM_003739
GPR64	G protein–coupled receptor 64	5′: CCAAAGAAA ATGTCAGGAAGCAATGG 3′: AGCAGTGTGGTGGAGTTAGTGGAG	NM_001079858.1
hK2	Human glandular kallikrein 2	5′: ATGTTGTGTGCTGGGCTCTGGAC 3′: GGTTGGC TGCGATCCTGTCCTTG	NM_005551
ODC 1	Ornithine decarboxylase 1	5′: ATGTGGGTGATTGGATGCTCTTTGA 3′: CAGGCTGCTCTGTGGCGTTTCAT	NM_002539
PSA	Prostate-specific antigen	5′: CCCCAGAATCACCCGAGCAG 3′: ACCAGAGGAGTTCTTGACCCCAAAA	NM_001648
SAA2	Serum amyloid A2	5′: TGCTCGGGGGAACTATGATGCTG 3′: GTCGGAAGTGATTGGGGTCTCTG	NM_030754
SRD5A1	Steroid-5-alpha-reductase, alpha polypeptide 1	5′: CCTGTTGAATGCTTCATGACTTG 3′: TAAGGCAAAGCAATGCCAGATG	NM_001047
RUNX1	Runt-related transcription factor 1	5′: CTCCCTGAACCACTCCACTGCCT 3′: GACCCACATTCTGCCTTCCTCATAA	NM_001001890

Table W2. Changes in Androgen-Regulated Genes by HE3235.

Gene Symbol	Gene Name	Fold Change
Increased expression		
SAA2	Serum amyloid A2	5.8
FER1L3	fer-1-like 3, myoferlin (*C. elegans*)	4.1
RUNX1	Runt-related transcription factor 1 (acute myeloid leukemia 1; *aml1* oncogene)	3.9
GPR64	G protein–coupled receptor 64	3.0
LOX	Lysyl oxidase	2.5
RIS1	Ras-induced senescence 1	2.5
PKNOX2	PBX/knotted 1 homeobox 2	2.3
RBM24	RNA binding motif protein 24	2.3
ABCG1	ATP-binding cassette, subfamily G (WHITE), member 1	2.2
GDF15	Growth differentiation factor 15	2.2
ODC1	Ornithine decarboxylase 1	2.2
TFF1	Trefoil factor 1 (breast cancer, estrogen-inducible sequence expressed in)	2.2
ABCC4	ATP-binding cassette, subfamily C (CFTR/MRP), member 4	2.1
CDH26	Cadherin-like 26	2.0
GDA	Guanine deaminase	2.0
CDC42EP2	CDC42 effector protein (Rho GTPase binding) 2	2.0
IL1R1	Interleukin 1 receptor, type I	2.0
FADS1	Fatty acid desaturase 1	2.0
PXDN	Peroxidasin homolog (*Drosophila*)	2.0
ChGn	Chondroitin beta1,4 *N*-acetylgalactosaminyltransferase	2.0
AZGP1	alpha-2-Glycoprotein 1, zinc	2.0
FABP5	Fatty acid binding protein 5 (psoriasis-associated)	1.9
S100A11	S100 calcium binding protein A11 (calgizzarin)	1.9
LOC114984	Hypothetical protein BC014089	1.9
MAF	v-*maf* musculoaponeurotic fibrosarcoma oncogene homolog (avian)	1.9
LGALS3	Lectin, galactoside-binding, soluble, 3 (galectin 3)	1.9
GPX3	Glutathione peroxidase 3 (plasma)	1.9
LOC645904	Similar to mitotic spindle assembly checkpoint protein MAD1 (mitotic arrest deficient-like protein 1) (MAD1-like 1) (mitotic checkpoint MAD1 protein-homolog) (HsMAD1) (hMAD1) (Tax-binding protein 181)	1.9
SAT	Spermidine/spermine N1-acetyltransferase	1.9
CASP10	Caspase 10, apoptosis-related cysteine peptidase	1.8
CRISP3	Cysteine-rich secretory protein 3	1.8
PPM1E	Protein phosphatase 1E (PP2C domain containing)	1.8
CTBP1	C-terminal binding protein 1	1.8
C15orf48	Chromosome 15 open reading frame 48	1.8
PGC	Progastricsin (pepsinogen C)	1.8
PVRL3	Poliovirus receptor-related 3	1.8
C21orf122	Chromosome 21 open reading frame 122	1.7
RPL36A	Ribosomal protein L36a	1.7
SLC26A2	Solute carrier family 26 (sulfate transporter), member 2	1.7
NFKBIZ	Nuclear factor of kappa light polypeptide gene enhancer in B-cells inhibitor, zeta	1.7
AGR2	Anterior gradient 2 homolog (*Xenopus laevis*)	1.7
MICAL1	Microtubule-associated monoxygenase, calponin and LIM domain containing 1	1.7
LFNG	Lunatic fringe homolog (*Drosophila*)	1.7
MRPL33	Mitochondrial ribosomal protein L33	1.7
AMPD3	Adenosine monophosphate deaminase (isoform E)	1.7
MGC33839	Hypothetical protein MGC33839	1.7
RPLP1	Ribosomal protein, large, P1	1.7
ZNF33A	Zinc finger protein 33A	1.6
AMACR	alpha-Methylacyl-CoA racemase	1.6
RPL21	Ribosomal protein L21	1.6
GRHL2	Grainyhead-like 2 (*Drosophila*)	1.6
SUMO2	SMT3 suppressor of mif two 3 homolog 2 (yeast)	1.6
RAB32	RAB32, member RAS oncogene family	1.6
C6orf166	Chromosome 6 open reading frame 166	1.6
MT1G	Metallothionein 1G	1.6
GNE	Glucosamine (UDP-*N*-acetyl)-2-epimerase/ *N*-acetylmannosamine kinase	1.6
POPDC3	Popeye domain containing 3	1.6
TIMP2	TIMP metallopeptidase inhibitor 2	1.6
CLDN8	Claudin 8	1.6
LIPG	Lipase, endothelial	1.6
RFPL1	Ret finger protein-like 1	1.6
LONPL	Peroxisomal LON protease like	1.6
ARHGEF10	Rho guanine nucleotide exchange factor (GEF) 10	1.6
RHOBTB3	Rho-related BTB domain containing 3	1.6
C14orf78	Chromosome 14 open reading frame 78	1.6
SAA3	Serum amyloid A3	1.6
FER1L4	Fer-1-like 3, myoferlin (*C. elegans*)	1.6
Decreased expression		
JUN	v-*jun* sarcoma virus 17 oncogene homolog (avian)	–1.6
IRX5	Iroquois homeobox protein 5	–1.6
SLC3A1	Solute carrier family 3 (cystine, dibasic and neutral amino acid transporters, activator of cystine, dibasic and neutral amino acid transport), member 1	–1.7
TFPI	Tissue factor pathway inhibitor (lipoprotein-associated coagulation inhibitor)	–1.7
JAG1	Jagged 1 (Alagille syndrome)	–1.9
CD44	CD44 antigen (Indian blood group)	–2.0
AR	Androgen receptor (dihydrotestosterone receptor; testicular feminization; spinal and bulbar muscular atrophy; Kennedy disease)	–3.1
AK5	Adenylate kinase 5	–3.7

Table W3. Steroidogenesis Enzymes.

Gene Symbol	Gene Name
AKR1C1	Aldo-keto reductase family 1, member C1 (dihydrodiol dehydrogenase 1; 20-alpha (3-alpha)-hydroxysteroid dehydrogenase)
AKR1C3	Aldo-keto reductase family 1, member C3 (3-alpha hydroxysteroid dehydrogenase, type II)
CYP11A1	Cytochrome P450, family 11, subfamily A, polypeptide 1
CYP17A1	Cytochrome P450, family 17, subfamily A, polypeptide 1
FASN	Fatty acid synthase
HSD17B1	Hydroxysteroid (17-beta) dehydrogenase 1
HSD17B2	Hydroxysteroid (17-beta) dehydrogenase 2
HSD17B3	Hydroxysteroid (17-beta) dehydrogenase 3
HSD17B4	Hydroxysteroid (17-beta) dehydrogenase 4
HSD17B6	Hydroxysteroid (17-beta) dehydrogenase 6
SRD5A1	Steroid-5-alpha-reductase, alpha polypeptide 1 (3-oxo-5 alpha-steroid delta 4-dehydrogenase alpha 1)
UGT2B15	UDP glucuronosyltransferase 2 family, polypeptide B15
UGT2B17	UDP glucuronosyltransferase 2 family, polypeptide B17